J. Math. Biol. (2013) 67:143–168
DOI 10.1007/s00285-012-0523-z

Mathematical Biology

Inverse problems from biomedicine

Inference of putative disease mechanisms and robust therapeutic strategies

James Lu · Elias August · Heinz Koeppl

Received: 31 August 2011 / Revised: 6 March 2012 / Published online: 18 April 2012

Abstract Many complex diseases that are difficult to treat cannot be mapped onto a single cause, but arise from the interplay of multiple contributing factors. In the study of such diseases, it is becoming apparent that therapeutic strategies targeting a single protein or metabolite are often not efficacious. Rather, a systems perspective describing the interaction of physiological components is needed. In this paper, we demonstrate via examples of disease models the kind of inverse problems that arise from the need to infer disease mechanisms and/or therapeutic strategies. We identify the challenges that arise, in particular the need to devise strategies that are robust against variable physiological states and parametric uncertainties.

Keywords Systems biology · Disease modeling · Inverse problems · Dynamical systems

Mathematics Subject Classification 92C42 · 97M60 · 65P30

J. Lu · E. August · H. Koeppl
Biomolecular Signaling and Control Group, Automatic Control Laboratory,
ETH Zurich, Zurich, Switzerland

E. August
e-mail: august@control.ee.ethz.ch

H. Koeppl
e-mail: koeppl@ethz.ch

Present Address:
J. Lu (✉)
Clinical Modeling & Simulation, Translational Research Sciences,
F. Hoffmann-La Roche, Basel, Switzerland
e-mail: james.lu.jl1@roche.com

1 Introduction

In recent years, there has been a shift away from the perspective of viewing diseases as isolated physiological dysfunctions towards a network view of pathogenesis (Liu and Lauffenburger 2009). There is an increasing awareness of the need for ushering in a era of "model-based medicine" to supplement evidence-based medicine (Zenker et al. 2007), including the use of biological knowledge together with patient-specific data in stratifying patients for personalized therapy (Faratian et al. 2009). Given a parametrized differential equations model of a disease, there has been a significant amount of research effort looking into the inference of optimal therapeutic strategies, ranging from: optimal drug administration (Lim and Teo 1989), chemotherapy (Swan 1984), multi-drug therapy (Magombedze et al. 2011), the control of the hypothalamic–pituitary–adrenal (HPA) axis for the correction of chronic stress syndrome (Ben-Zvi et al. 2009), the control of glucose regulation in diabetic patients (Acikgoz and Diwekar 2010) and the identification of optimal drug combinations in signaling and metabolic networks (Iadevaia et al. 2010; Yang et al. 2008).

However, much of the existing literature do not take into account the ill-posedness inherent in the process of diagnosis (Zenker et al. 2007) as well as the subsequent identification of appropriate therapeutic strategies (Yang et al. 2008). In particular, the traditional approach of identifying an optimal solution under a given physiological state and an assumed set of parameter values may give rise to misleading results that fail to be consistent with the outcomes of clinical tests. The inaccuracy of model predictions for disease treatments may arise from some combination of the following factors:

- the relevant biology may not be completely known: for instance, in cancer models not all of the relevant oncogenes and tumor suppressor nodes in the relevant signaling pathway may have been found, giving rise to incomplete network topologies;
- given a network of fine granularity and broad coverage, the interaction strengths of pathways components often cannot be fully determined from the available data, resulting in parametric uncertainties due to the lack of practical or structural identifiability (Miao et al. 2011);
- the physiological states may vary significantly between individuals as well as between cell types;
- drugs that affect the desired physiological process may also have unknown side-effects, restricting their therapeutic windows.

These factors pose significant challenges to the use of modeling in biomedicine. In order to counteract the lack of complete knowledge and quantitative data, we propose the following set of strategies:

- formulation of inverse problems involving qualitative dynamics when detailed quantitative knowledge is lacking;
- solving the robust counterpart of optimal treatment strategies when problem uncertainties become important;
- application and development of appropriate regularization methods in managing problem dependent side-effects and ill-posedness.

In Sect. 2, we propose inverse analysis of qualitative dynamics as a way to illuminate the task of disease treatment even when quantitative time-course data is not readily available. This section serves to motivate the focus of the paper on qualitative dynamics. In Sect. 3, we show some links between robustness and its approximations via regularization strategies and propose some methods for treating identification problems under uncertainties. Results in this direction show that while the general robust optimization problem is computationally challenging, one way to construct surrogate approximations that approach the robustified version is via the use of regularization methods. In Sect. 4, we show some illustrative examples of inverse problems in disease identification and treatments, with the main goal being examining the effect of different regularization strategies and their possible implications on solution robustness and sparsity. Finally, given that we have only taken the first steps in showing some correspondence between robustness criteria and regularization and much remains to be developed and understood, in Sect. 5 we point to some of the new challenges that arise in tackling inverse problems from biomedicine.

2 Inverse problems for qualitative dynamics

Let us denote the dynamical system of interest as

$$\dot{x}(t) = f(x(t), \alpha, \gamma), \tag{1}$$

where $\alpha \in \mathbb{R}^m$ is the set of kinetic and physiological parameters, $\gamma \in \mathbb{R}^r$ are the set of bifurcation or input parameters of interest. The distinction between these two classes of parameters is usually made on a problem- and task-dependent basis; kinetic parameter are those that play a role in regulating the system dynamics, while input parameters are those that are primarily not under the control or regulation of the system under study but to which the latter should respond in accordance. For instance, in signaling models γ may play the role of ligand concentration that triggers a switch in response.

As an example of a qualitative inverse problem (Lu et al. 2006; Engl et al. 2009), let us consider the task of relocating the positions of limit-point bifurcation points (Kuznetsov 2004) in a bistable switch system. While the transient dynamics may be important for some biological phenomena, in many instances the steady-state behavior discriminates between healthy and diseased states. For bifurcation points occurring at abscissas γ_1, γ_2 (see Fig. 1 for an illustration), the system satisfies the following conditions:

$$\begin{aligned} &f(x, \alpha, \gamma_1) = f(x, \alpha, \gamma_2) = 0 \\ &\det\left(\frac{\partial f}{\partial x}(x, \alpha, \gamma_1)\right) = \det\left(\frac{\partial f}{\partial x}(x, \alpha, \gamma_2)\right) = 0. \end{aligned} \tag{2}$$

Note that in Fig. 1 only a single state variable is plotted, while the state of the system would almost always be multi-dimensional; in particular, x represents a measurable biomarker of the system whose level is indicative of the healthy versus diseased states.

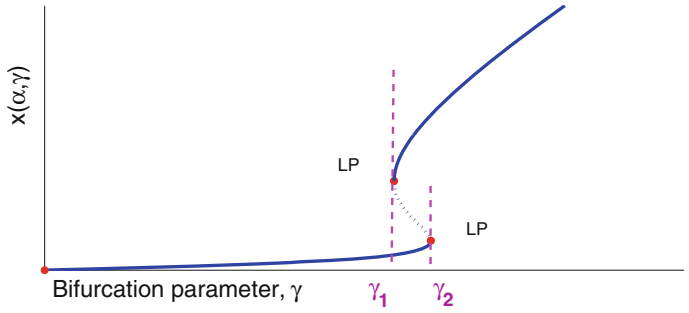

Fig. 1 Illustration of a bistable system with 2 limit-point bifurcation points

In posing qualitative inverse problems, we assume that the input values at which the system switches between states (i.e., γ_1, γ_2 in Fig. 1) and the relevant state component indicative of such a switching can be measured; however, the kinetic parameters and whole set of state variables need not be known. The locations of bifurcation points of a biological system often have direct relevance to the physiological state and the need to solve inverse problems associated with the geometry of bifurcation manifolds arise in many situations:

- in modeling, the values of the input signal at which the system dynamics changes in a qualitative manner may lead to valuable constraints for the model parameters (Cedersund and Knudsen 2005);
- in trying to identify putative mechanisms underlying observed dynamic diseases (Glass and Mackey 1979), solving inverse qualitative problems may allow one to explore different hypotheses;
- in attempting to devise possible therapeutic strategies for diseases associated with the control system crossing into an undesired dynamical regime, the optimal intervention strategies for remedying the disease can be obtained solving the associated inverse problems (Engl et al. 2009).

Given a dynamical system let $F(\cdot)$ denote the (forward) operator that maps a parameter set to the bifurcation structure, Γ. In the bistable example discussed here, the bifurcation structure of interest could consist of the vector of abscissas for the two bifurcation points, $\Gamma = (\gamma_1, \gamma_2)$; more generally, Γ may encode the geometry of the bifurcation. Given a desired bifurcation structure Γ^*, starting from the (uncertain) nominal parameter values α^0, the inverse qualitative problem may be formulated in a general manner as the following nonlinear operator equation: find $\alpha^* \in \mathbb{R}^m$ such that,

$$F(\alpha^*) = \Gamma^*. \tag{3}$$

Once the α^* has been derived, its difference from the nominal $\alpha^* - \alpha^0$ represents the desired parameter change that one would wish to obtain from the pharmacological intervention. For implementation details, see Lu et al. (2006) for a discussion on gradient-based methods that move bifurcation points to desired locations. We remark that in general, the inverse problem (3) suffers from the effects of ill-posedness (Engl et al. 1996); for applications in biomedicine, the following are of special importance:

- the identified solution α^* may be sensitive to perturbations $\delta\alpha$: that is, $\|F(\alpha^* + \delta\alpha) - \Gamma^*\|/\|\delta\alpha\| \gg 1$;
- many solutions α^* may exist, in which case one needs to select those out of the solution set that are of the most interest: they are usually solutions involving few non-zero components in $\alpha^* - \alpha^0$, where α^0 is the nominal parameter set that matches the nominal data/dynamics. Typically, sparse solutions can be more easily checked experimentally or implemented as therapeutic strategies.

Therefore, one needs to apply and develop appropriate methods that can find the desired balance between robustness and sparsity in the solutions to the inverse problems.

3 Regularization strategies

3.1 Incorporating robustness

We consider the problem of starting with a model that exhibits the nominal dynamical characteristics (denoted as Γ^0) and we wish to identify a parameter set that gives rise to the desired dynamics. In particular, due to the typical paucity of data in problems of biomedicine we do not assume the parameters are identifiable (Miao et al. 2011) and hence wish to account for the uncertainty in the nominal parameters. As stated in Sect. 2, we assume the values of input parameters are known as well as component(s) of the state which allows for the characterization of qualitative system dynamics. From these and any additional quantitative data for the system, using parameter identification methods we assume that at least one single parameter set α^0 has been found that matches the data up to a δ-tolerance, the estimated noise level. Hence, in terms of the operator formalism described in Sect. 2, we have: $\|F(\alpha^0) - \Gamma^0\| \leq \delta$. However, typically α^0 is not the only parameter set matching the given data: we denote by $\mathcal{D}(\delta)$ the set of all parameters matching the nominal dynamics up to δ-tolerance. By definition, $\alpha^0 \in \mathcal{D}(\delta)$ and,

$$\|F(\alpha) - \Gamma^0\| \leq \delta, \quad \forall \alpha \in \mathcal{D}(\delta). \tag{4}$$

For the purpose of developing tight bounds below, ideally α^0 should be close to the centroid of the region $\mathcal{D}(\delta)$.

Now we consider the inverse problem of identifying an α^* that is mapped, via $F(\cdot)$, to the desired dynamical characteristics Γ^*. Note that the initial uncertainty region $\mathcal{D}(\delta)$ is mapped to the identified parameter, giving rise to the parametric uncertainty of the form $\alpha^* + (\tilde{\alpha} - \alpha^0)$ where $\tilde{\alpha} \in \mathcal{D}(\delta)$. In the estimates derived below, we make the assumption that the desired Γ^* is significantly beyond the initial uncertainty level, $\|\Gamma^* - \Gamma^0\| \gg \delta$, hence a non-trivial parameter change is needed to bring about the desired system dynamics.

In the idealized situation of no data noise and parametric uncertainties, we could well identify the parameter change $\alpha^* - \alpha^0$ corresponding to a disease mechanism or therapeutic strategy that underly or result in Γ^* respectively, by simply solving the following minimization problem:

$$\alpha^* \leftarrow \arg\min_{\alpha \in \mathbb{R}^m} \|F(\alpha) - \Gamma^*\|. \tag{5}$$

First of all, even in the stated idealized situation the solution α^* may not be unique; however, this usually does not pose a major impediment as one can simply select the desirable ones from the identified solution set. A more important consideration is the robustness (Hafner et al. 2009) of the solution:

- for the application of identifying putative disease mechanisms, it is likely that the diseased state persists under variable physiological states;
- for identifying therapeutic strategies, one would like the intervention approach to be effective under variable drug concentrations as well as various cell types.

This motivates us to solve the *robust counterpart* (Ben-Tal et al. 2009) to (5):

$$\alpha^*_{RC} \leftarrow \arg\min_{\alpha \in \mathbb{R}^m} \max_{\tilde{\alpha} \in \mathcal{D}(\delta)} \|F(\alpha + (\tilde{\alpha} - \alpha^0)) - \Gamma^*\|, \tag{6}$$

where $\tilde{\alpha}$ is used to denote variations in the kinetic parameters, due to incomplete knowledge. We define $J_{RC}(\alpha) \equiv \max_{\tilde{\alpha} \in \mathcal{D}(\delta)} \|F(\alpha + (\tilde{\alpha} - \alpha^0)) - \Gamma^*\|$ as the robustified objective function, the evaluation of which, in general, involves sampling over parameter sets. Below, we develop a bound for $J_{RC}(\alpha)$ and show how an approximation of the robust version has a correspondence with variational regularization.

We assume that $F(\cdot)$ is differentiable, hence by the mean-value theorem applied to the path between $\tilde{\alpha}$ and $(\alpha - \alpha^0) + \tilde{\alpha}$ we have:

$$F((\alpha - \alpha^0) + \tilde{\alpha}) = F(\tilde{\alpha}) + \left(\int_0^1 \nabla F(\tilde{\alpha} + c(\alpha - \alpha^0)) dc \right) \cdot (\alpha - \alpha^0). \tag{7}$$

Therefore, using the error bound (4) and triangle inequality, we have the following bound for the expression contained in (6),

$$\begin{aligned} &\forall \tilde{\alpha} \in \mathcal{D}(\delta): \\ &\|F(\alpha + (\tilde{\alpha} - \alpha^0)) - \Gamma^*\| \\ &\quad \leq \delta + \left\| \left(\int_0^1 \nabla F(\tilde{\alpha} + c(\alpha - \alpha^0)) dc \right) \cdot (\alpha - \alpha^0) - (\Gamma^* - \Gamma^0) \right\|. \end{aligned} \tag{8}$$

Let us examine the part of the above bound which has dependence on the parameter uncertainty, $\tilde{\alpha} \in \mathcal{D}(\delta)$. Define the uncertainty range of the Jacobian matrix as:

$$\mathcal{U}(\alpha) \equiv \left\{ \int_0^1 \nabla F(\tilde{\alpha} + c(\alpha - \alpha^0)) dc \mid \tilde{\alpha} \in \mathcal{D}(\delta) \right\}. \tag{9}$$

Using the above, we have an upper-bound for $J_{RC}(\alpha)$ as defined in (6):

$$J_{RC}(\alpha) \leq \delta + \max_{A \in \mathcal{U}(\alpha)} \|A \cdot (\alpha - \alpha^0) - (\Gamma^* - \Gamma^0)\|. \tag{10}$$

Since $\alpha^0 \in \mathcal{D}(\delta)$, by the mean-value theorem, $\bar{A}(\alpha, \alpha^0) \equiv \int_0^1 \nabla F(\alpha^0 + c(\alpha - \alpha^0))dc \in \mathcal{U}(\alpha)$ satisfies the following:

$$\bar{A}(\alpha, \alpha^0) \cdot (\alpha - \alpha^0) = F(\alpha) - F(\alpha^0). \tag{11}$$

Define $\rho(\alpha)$ as an upper bound for the Frobenius distance between members of the set $\mathcal{U}(\alpha)$ and $\bar{A}(\alpha, \alpha^0)$: $\|u - \bar{A}(\alpha, \alpha^0)\|_F \leq \rho(\alpha), \forall u \in \mathcal{U}(\alpha)$. Using the above and appealing to a result of robust least-squares (El Ghaoui and Lebret 1997), $J_{RC}(\alpha)$ of (6) may be bounded by:

$$\begin{aligned} J_{RC}(\alpha) &\leq \delta + \max_{A \in \{\bar{A}(\alpha,\alpha^0) + \tilde{A} \mid \|\tilde{A}\|_F \leq \rho(\alpha)\}} \|A \cdot (\alpha - \alpha^0) - (\Gamma^* - \Gamma^0)\| \\ &\leq \delta + \|\bar{A}(\alpha, \alpha^0) \cdot (\alpha - \alpha^0) - (\Gamma^* - \Gamma^0)\| + \max_{\{\tilde{A} \mid \|\tilde{A}\|_F \leq \rho(\alpha)\}} \|\tilde{A} \cdot (\alpha - \alpha^0)\| \\ &\leq 2\delta + \|F(\alpha) - \Gamma^*\| + \max_{\{\tilde{A} \mid \|\tilde{A}\|_F \leq \rho(\alpha)\}} \|\tilde{A} \cdot (\alpha - \alpha^0)\| \\ &= 2\delta + \|F(\alpha) - \Gamma^*\| + \rho(\alpha)\|\alpha - \alpha^0\|. \end{aligned} \tag{12}$$

In conclusion, we have shown that if the Jacobian uncertainty set $\mathcal{U}(\alpha)$ is well-approximated by $\{\bar{A}(\alpha, \alpha^0) + \tilde{A} \mid \|\tilde{A}\|_F \leq \rho(\alpha)\}$, solving the robust counterpart of the uncertain inverse problem corresponds to a applying a variational regularization. If this assumption does not hold but $\mathcal{U}(\alpha)$ is better approximated by some other convex set, then the robustness criterion would have correspondence to some other form of variational regularization; we leave this as an open problem for future work.

We remark that there are other ways to "immunize against uncertainty" (Ben-Tal et al. 2009) in solving inverse problems. As an alternate to the robust optimization formulation given in (6), one can take a stochastic optimization approach (Stengel 1986; Hafner et al. 2011) and minimize the expected value of the mis-match:

$$\alpha^*_{SO} \leftarrow \arg\min_{\alpha \in \mathbb{R}^m} \mathrm{E}_{\tilde{\alpha}}[\|F(\alpha + \tilde{\alpha}) - \Gamma^*\|]. \tag{13}$$

Parameter distributions for $\tilde{\alpha}$ (that match the known data) may be obtained by using Bayesian inference, for instance. The stochastic approach is less conservative than the robust formulation, the trade-off being that one should be willing to accept probabilistic guarantees.

3.2 Minimal-norm and sparsity

In addition to the use of a robust formulation to account for model uncertainties, a strictly convex variational regularization term can be appended for additional stability

in order to counteract the effect of data noise. A standard regularization method is to include the l_2-norm as the penalty term, which gives rise to Tikhonov regularization (Engl et al. 1996):

$$\alpha^* \leftarrow \arg\min_{\alpha\in\mathbb{R}^m} \|F(\alpha) - \Gamma^*\|^2 + \mu\|\alpha - \alpha^0\|_2^2. \tag{14}$$

For examples showing the effect of stabilization in parameter estimation for biochemical networks, refer to Engl et al. (2009).

Regularization methods based on the l_1-norm can be useful under the assumption that the underlying network is sparse (August and Papachristodoulou 2009), that is consisting of few non-zero edges. The identification of sparse vectors can also be useful in pinpointing important factors underlying the observed effects; for instance, in cluster analysis on microarray data, sparsity helps to identify the key genes out of the many (d'Aspremont et al. 2007). For linear problems, under the condition that a sufficiently sparse solution exists, it has been shown that l_1 minimization can give good approximations to the sparsest solution (Donoho 2006). However, for highly nonlinear problems, a non-convex regularization term may be necessary to identify sparse solutions (Engl et al. 2009). In particular, the following sparsity-promoting penalty has been proposed:

$$l_{p,\epsilon}(x) \equiv \sum_{i=1}^{n} (x^2 + \epsilon)^{p/2}, \quad 0 < p < 1. \tag{15}$$

Despite the fact that there has been some theoretical underpinnings for the use of such a non-convex regularization term (Zarzer 2009), much remain to be understood in terms of their stabilizing properties.

Elastic net is a regularization method that combines l_2 and l_1 penalties to identify sparse groups of correlated features (Zou and Hastie 2005). Methods based on mixing penalty functions have been used in a number of biological applications, including network inference (Shimamura et al. 2009) and gene selection from microarray data (De Mol et al. 2009). We propose an extension of the use of elastic-net methodology to nonlinear problems, by combining the l_2 with sparsity-enforcing $l_{p,\epsilon}$-function: that is, we seek,

$$\alpha^* \leftarrow \arg\min_{\alpha\in\mathbb{R}^m} \|F(\alpha) - \Gamma^*\|^2 + \mu\|\alpha - \alpha^0\|_2^2 + \mu_s l_{p,\epsilon}(\alpha - \alpha^0). \tag{16}$$

In order to obtained desired solution properties, one needs to find the appropriate balance between the regularization parameters, μ and μ_s. We expect that in practical applications, there is likely not be a single criterion on the desired trade-off between sparsity and the norm of the solution; instead, the user of the identification algorithm may wish to obtain a sequence of solutions from which candidate strategies are then selected based on their feasibility. We currently do not have a way to select regularization parameters based on some plausible user criteria and leave this to future work.

3.3 Applications to biomedicine

Amongst the applications of inverse problems to biomedicine, we consider the following:

1. inferring disease mechanisms underlying the observed diseased phenotype;
2. identifying intervention strategies given a diseased phenotype.

In case 1, one wishes to infer the most likely and simplest cause, out of the many that would all give rise to the same observed diseased state. While many combinations of kinetic rates in the physiological system may have changed due to genetic and environmental factors, one may assume that the different instances of the disease may arise from a few important sparse factors. Therefore, sparsity enforcing penalty would have more relevance in this case. In case 2, there is typically no *a priori* restriction in the number of drug combinations used; however, the drug dosage should be controlled in order to avoid toxicity, especially those drug combinations that give rise to synergistic adverse effects. Therefore, in such applications the minimal-norm penalty would generally have a higher priority. In addition, a symmetric positive definite weight matrix W may be introduced in order to penalize any known drug combination toxicity effects.

In summary, for inferring the best therapeutic strategies one may wish to find an appropriate trade-off between high degree of robustness, against low toxicity and sparsity by an appropriate tuning of the respective penalty parameters μ_t and μ_s:

$$\begin{aligned}\alpha^* \leftarrow \arg\min_{\alpha\in\mathbb{R}^m} \max_{\tilde{\alpha}\in\mathcal{D}(\delta)} \|F(\alpha + (\tilde{\alpha} - \alpha^0)) - \Gamma^*\|^2 \\ +\mu_t(\alpha - \alpha^0)^T W(\alpha - \alpha^0) + \mu_s l_{p,\epsilon}(\alpha - \alpha^0).\end{aligned} \tag{17}$$

We remark that while (17) formulates the robustness problem in the general setting, further work is needed to make it a computationally tractable task. In order to render the minimization problem implementable, one needs to approximate $\mathcal{D}(\delta)$ or optimize a surrogate function for (17). Also needed is a method of determining the regularization parameters in relation to the desired level of robustness.

4 Examples

In this section, we consider inverse problems for a number of examples from the systems biology and disease modeling literature. The aim here is not to draw particular implications from the results of the inverse analysis, but to show what type of inverse problems of qualitative nature may arise and what computational methodologies can be applied. We remark that there may be no single computational approach which can be used for solving all such problems in one go; instead, the solution process is likely to be iterative in nature and involve a combination of computational approaches. In particular, the steps may involve first evaluating the robustness of the identified (regularized) solutions and certify the level of robustness if possible. If the solution robustness of the solution needs to be improved, more computationally intensive procedures can then be called upon to find the desired trade-off between solution magnitude, sparsity and robustness. In Sect. 4.1, we demonstrate how the use of sparsity

regularization identifies a solution that suggests the plausibility of the proposed disease mechanism. In Sect. 4.2, we use the sum of squares (SOS) technique to provide a certificate on the solution robustness and compare it to numerical estimates. In Sect. 4.3, we employ elastic net regularization to identify a sequence of solutions of decreasing sparsity, which could be different in their robustness against resistance mechanisms.

4.1 HPA axis: cyclic Cushing syndrome

The hypothalamic–pituitary–adrenal (HPA) axis is a neuroendocrine system which plays a key role in governing homeostasis of the human body in response to various stresses (Gupta et al. 2007). Under normal physiological conditions, stress triggers the hypothalamus to release corticotropin releasing hormone (CRH), which travels via the blood circulation and in turn activates the secretion of adrenocorticotropic hormone (ACTH) in the pituitary. ACTH stimulates the adrenals to synthesize and secrete cortisol, which binds with the gluococorticoid receptors (GR) and feedback negatively on both the hypothalamus and pituitary in their secretion of CRH and ACTH respectively.

A mathematical model of the HPA axis has been proposed by Gupta et al. (2007), showing that the system is able to exhibit bistable behavior, with the switching between states triggered by changes in the stress level. The model consists of 3 organs (namely, the hypothalamus, pituitary and adrenals) with the production and degradation of the respective hormones described by linear kinetics. Michaelis–Menten enzyme kinetics is used to capture the inhibitory effect of cortisol, while Hill kinetics is used in describing the up-regulation of glucocorticoid receptors in the pituitary following the binding of cortisol. The system of equations is shown below,

$$\begin{aligned}
\frac{d}{dt}[ACTH] &= K_a \frac{[CRH]}{\frac{[cortisol][GR]}{K_{i2}} + 1} - K_{ad}[ACTH] \\
\frac{d}{dt}[cortisol] &= K_o[ACTH] - K_{od}[cortisol] \\
\frac{d}{dt}[CRH] &= \frac{stress(t) + K_c}{\frac{[cortisol]}{K_{i1}} + 1} - K_{cd}[CRH] \\
\frac{d}{dt}[GR] &= K_r \frac{[cortisol]^2[GR]^2}{[cortisol]^2[GR]^2 + K} - K_{rd}[GR] + K_{cr}
\end{aligned} \tag{18}$$

The model predicts that upon transient stress of sufficiently short duration, the HPA system responds accordingly and return to the normal steady state following the removal of stress. However, upon stress inputs of a sufficiently long duration and/or magnitude, the glucocorticoid receptor synthesis remains turned on after the stress removal, leading to the chronic stress condition (Gupta et al. 2007). The transient and irreversible nature of stress response in the HPA axis are shown in Figs. 2 and 3 respectively.

Using this coarse-grained model of interaction between hormones and their secreting organs, one could already ask if known diseases can be mapped to the existing physiological knowledge as encoded in the model. One disease involving abnormal levels of

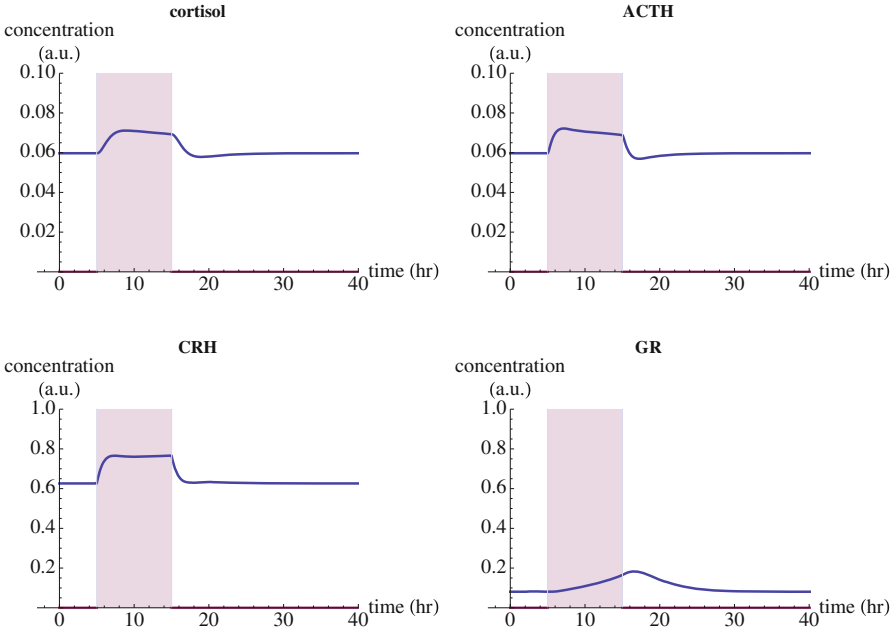

Fig. 2 Transient response of HPA axis to short duration stress

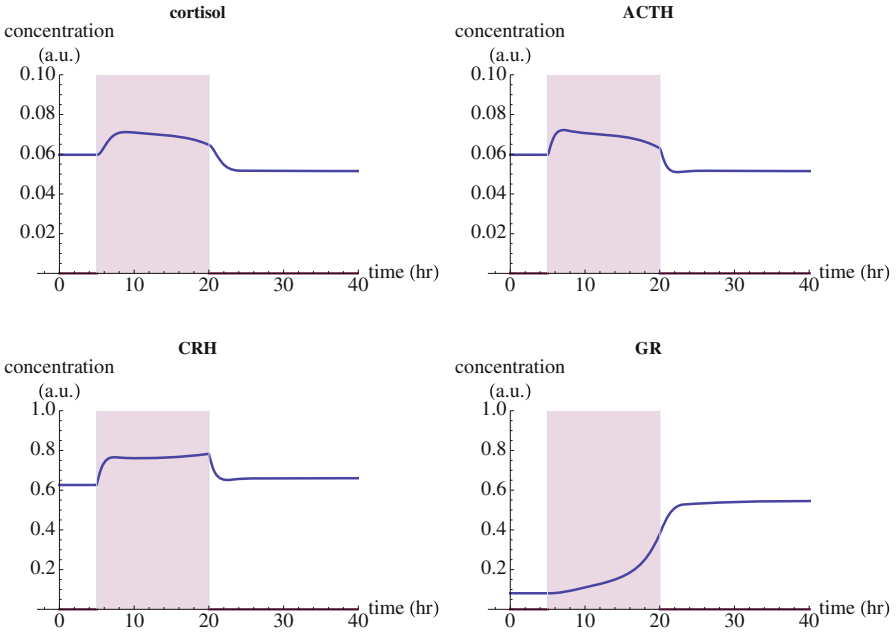

Fig. 3 Irreversible response of HPA axis to long duration stress

Table 1 Parameter change leading to oscillatory behavior in HPA axis model obtained using inverse eigenvalue analysis

Parameter	Affected reaction mechanism	Change
K_{od}	Degradation rate of cortisol	$1.0 \rightarrow 0.1104$
K_{i2}	Michaelis–Menten constant in inhibition of ACTH production by cortisol-glucocorticoid receptor complex	$0.1 \rightarrow 0.01$
K	Disassociation constant in the binding of glucocorticoid receptor dimers to its promoter	$0.001 \rightarrow 0.00354$

cortisol is the cyclic Cushing syndrome (CS) (Velez et al. 2007), where cortisol levels are seen to fluctuate in a cyclic manner, with durations ranging from 12 hours to days. Due to its periodic nature, the diagnosis of the cyclic CS can be easily missed if only a few measurements are taken. A long period of surveillance as well as a careful evaluation of the clinical data is necessary for a confirmation of the disease in terms of its signature troughs and peaks in the patient's cortisol level (Velez et al. 2007). The origins of cyclic CS is not well understood, although it could be related to corticotrophic adenoma of the pituitary, as well as with adrenal hyperplasia and hypothalamic disorders. As we have seen, the model has been shown to exhibit a bistable switching behavior (Gupta et al. 2007); from the need to understand putative mechanisms underlying cyclic CS, we ask: can the model also be made to exhibit oscillations by changing some of its parameters, as would be the case if some of the underlying physiological processes become dysfunctional?

In order to explore this question, we solve an inverse eigenvalue problem (see Lu 2009 for algorithmic details) to bring the system close to a Hopf bifurcation. For this task, the forward operator $F(\cdot)$ maps the kinetic parameters in the HPA model to the position of the eigenvalue pairs closest to the imaginary axis. The sparsity-enforcing penalty term $l_{p,\epsilon}$ was used, with $p = 1/10$, $\epsilon = 0.05^2$. The gradient-based optimization algorithm identified a change in only 3 out of the 12 model parameters, see Table 1 for the changes in model parameters; the remaining parameters each changed less than 5 % from its original value. The fact that only few parameters need to be varied and that changes are within an order of magnitude suggests that it is not implausible that physiological perturbations can bring about the diseased state. Figure 4 shows the oscillatory dynamics exhibited by the model using the identified parameters. While the posed problem is to bring about a limit cycle solution, due to the use of regularization term the condition $F(\alpha^*) = \Gamma^*$ is not exactly met and the system is brought to a damped oscillatory regime. However, numerical bifurcation analysis around the identified parameter values shows that the system can be brought to exhibit limit cycle oscillations. This inverse analysis shows that the known qualitative dynamics of cyclic CS is not in contradiction to the existing physiological knowledge. Therefore, mutations or other processes may affect kinetic parameters in such a way so as to give rise to oscillatory dynamics. Whether the identified combination of mechanisms are the minimal ones and how sensitive the oscillatory dynamics is with respect to parameter variations, remain topics for future work.

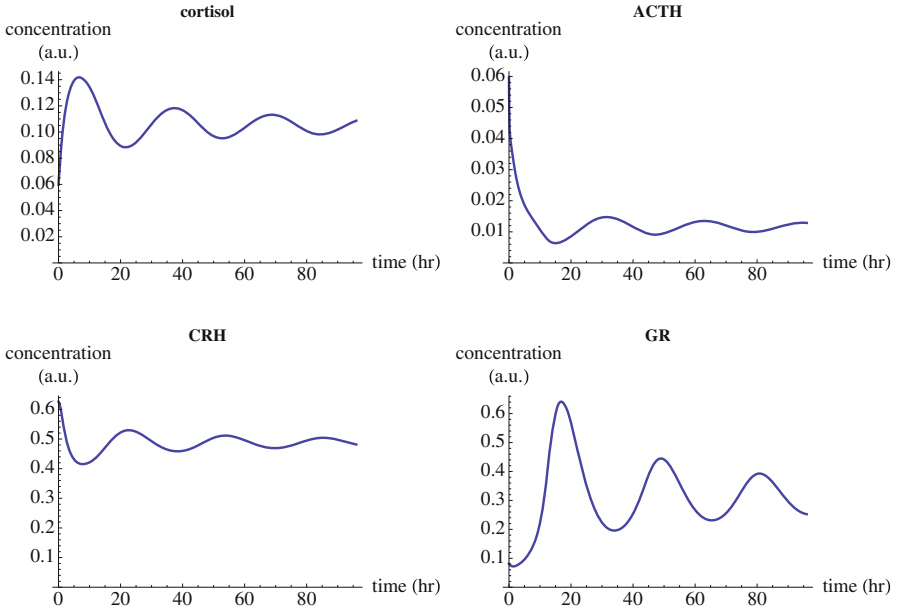

Fig. 4 Oscillatory dynamics in the HPA axis model using the identified parameter set

4.2 Lipoprotein metabolism

4.2.1 Model description

Lipoproteins are the primary means of transport of necessary lipids from the liver to the cells. Unfortunately, there is a strong body of medical evidence that when in excess in the blood stream, lipoproteins lead to the development of *atherosclerosis*, particularly if concentrations of low density lipoproteins (LDL) are high (Glass and Witztum 2001; Rodríguez et al. 1999; Libby 2002). Although much research has been carried out in this area, it is still unknown why plasma cholesterol concentrations in adults are so high (Goldstein and Brown 1977), what the exact effects of statins are (Davidson and Jacobson 2001), and which metabolic processes should be targeted to reduce plasma LDL concentrations most effectively. In the following, we provide a brief description of the main processes related to lipoprotein metabolism.

The liver secretes very low density lipoprotein (VLDL), whose rate we denote by u_V. While in the blood stream, VLDL is degraded by interaction with LPL (lipoprotein lipase) to intermediate density lipoprotein (IDL), which is then degraded in a similar fashion and forms LDL. We denote the turnover rates of VLDL and IDL in the blood stream by k_V and k_I, respectively. The uptake of lipoproteins by cells is mostly receptor-mediated. We denote the rate constants of the receptor-mediated uptake of LDL and IDL by d_L and d_I, respectively. It is also possible for LDL (but not for IDL) to be absorbed directly through a non-receptor mediated pathway (with rate constant d). Upon internalization, the lipoproteins are hydrolyzed in the cell releasing lipids into the cytoplasm. A significant proportion of these lipids (we denote these proportions

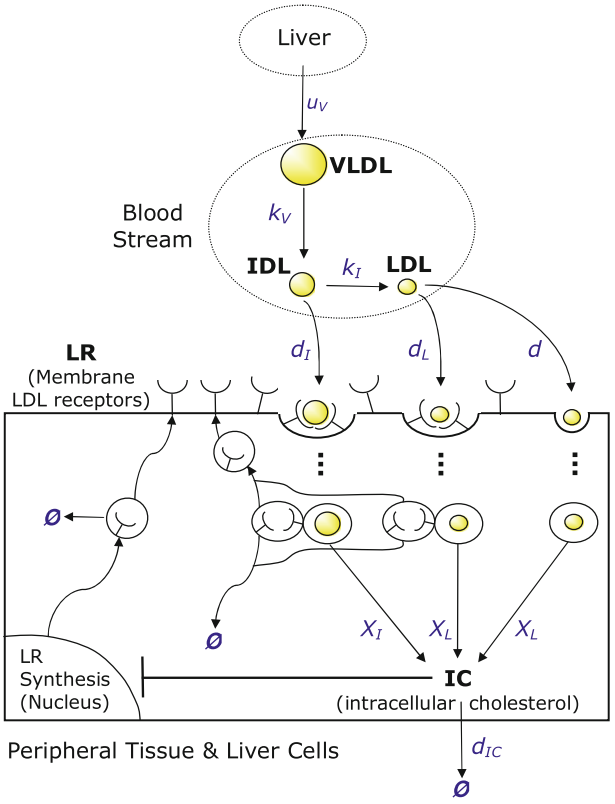

Fig. 5 Overview of origin, transport and fate of lipoproteins. The liver secretes VLDL, which goes into the bloodstream and is degraded by LPL to IDL. In turn, IDL is degraded to LDL. Cells take up lipoproteins in a receptor-mediated manner as well as directly

by χ_I and χ_L) is cholesterol which contributes to the level of intracellular cholesterol (IC). The intracellular cholesterol is used for cell function or eliminated, mainly through the action of high density lipoprotein (HDL), at a rate that we denote d_{IC}. Thus, HDL, which is also secreted by the liver, is the so called "good cholesterol", as it is responsible for *reverse cholesterol transport*, the transport of excess cholesterol from cells and from other lipoproteins back to the liver. Finally, a fraction $(1 - b)$ of receptors used in endocytosis is recycled and reincorporated into the membrane. In addition, the nuclear synthesis of receptors LR is regulated through negative feedback ($\vdash$) by intracellular cholesterol. Although almost every cell can synthesize cholesterol to some extent, we assume that all cholesterol has to be delivered to the cells via LDL or IDL absorption (Mathews et al. 2000; Cooper 2000; Converse and Skinner 1992; Dietschy et al. 1978). Figure 5, taken from reference (August et al. 2007), provides a schematic overview of the origin, transport and fate of the different lipoproteins in the human body.

In the following, we present a model of lipoprotein metabolism from reference (August et al. 2007), which exhibits a transition between low and high LDL steady states. Due to the fact that the equations are directly related to physiological

Table 2 Parameters of the model (19)

	Source	Units	Nominal value	Range
Kinetic parameter				
k_V	Packard et al. (2000)	h^{-1}	0.3	0.15–0.6
k_I	Packard et al. (2000)	h^{-1}	0.1	0.025–0.1
d_I	Packard et al. (2000)	h^{-1}	1.4	0.5–2
d_L	White and Baxter (1984)	h^{-1}	0.0075	0.005–0.02
d	Dietschy et al. (1993)	h^{-1}	0.0025	0.0025-0.0075
b	August et al. (2007)	lg^{-1}	0.1	0–1
c	Goldstein and Brown (1977)	$g(lh)^{-1}$	0.05	0–1
χ_I	Adiels (2002)	–	0.35	0.25–0.45
χ_L	Adiels (2002)	–	0.45	0.4–0.5
Control parameter				
u_V	White and Baxter (1984)	$g(lh)^{-1}$	0.3	Variable
d_{IC}	White and Baxter (1984)	h^{-1}	0.45	Variable

Nominal values and ranges as found in the literature. Because of their high dependence on diet, medication and genetics, we consider u_V and d_{IC} as the control parameters

processes, the model can be used to study the effect of medical or behavioral interventions. The previously described metabolic processes are modeled by the following system of differential equations, where $[\cdot]$ denotes concentration in g/l (August et al. 2007):

$$\begin{aligned}
\frac{d[VLDL]}{dt} &= -k_V[VLDL] + u_V \\
\frac{d[IDL]}{dt} &= k_V[VLDL] - k_I[IDL] - d_I[IDL]\phi_{LR} \\
\frac{d[LDL]}{dt} &= k_I[IDL] - d_L[LDL]\phi_{LR} - d[LDL] \\
\frac{d\phi_{LR}}{dt} &= -b\left(d_I[IDL] + d_L[LDL]\right)\phi_{LR} + c\frac{1-\phi_{LR}}{[IC]} \\
\frac{d[IC]}{dt} &= \left(\chi_I d_I[IDL] + \chi_L d_L[LDL]\right)\phi_{LR} + \chi_L d[LDL] - d_{IC}[IC]
\end{aligned} \tag{19}$$

Here, the attachment of the cytosolic LDL receptors to the cell surface is described in its simplest form with a rate that is proportional to the fraction of unoccupied receptor sites $(1-\phi_{LR})$. The combined rate at which ϕ_{LR} increases is then given by the product $c(1-\phi_{LR})/[IC]$, where parameter c modulates the weight of the combined process of regulated synthesis and attachment. The model contains 9 kinetic parameters and 2 control parameters u_V, d_{IC} with nominal values and ranges shown in Table 2.

We note that of the two control parameters, u_V can be more easily varied over individuals within a given population. Shown in Fig. 6 is the bifurcation diagram of

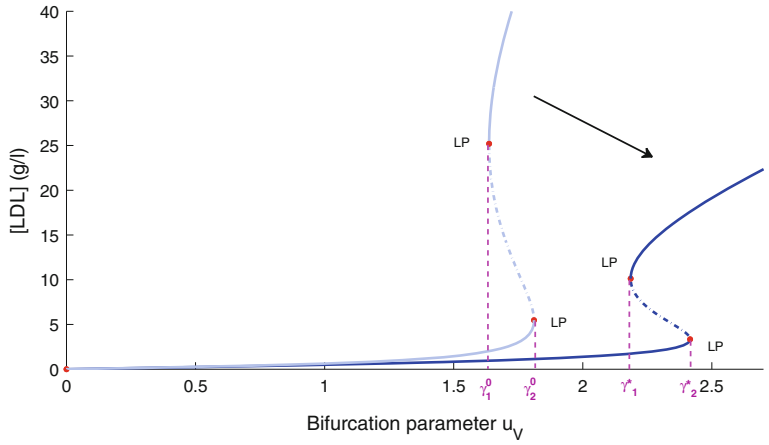

Fig. 6 The nominal bifurcation diagram (*curve* shown with lighter *shading*) with limit-points at the values of bifurcation parameter $u_V = \gamma_1^0, \gamma_2^0$ and a bifurcation diagram having the corresponding values at the desired locations, γ_1^* and γ_2^*

the lipoprotein model with u_V as the bifurcation parameter. The diagram shows that while for $u_V < \gamma_1^0 = 1.637$ the system has a single steady-state, within the range $\gamma_1^0 < u_V < \gamma_2^0$ the system can be in one of the two steady-states, depending on the history of the system trajectory and perturbations exerted on the system. Physiologically, this implies that individuals, who have higher values of u_V (due to diet or genetic factors), could suffer from the adverse condition of high LDL level in their system. Given the connection between the diseased state corresponding to high LDL and the bifurcation points of the model, for the purpose of identifying mechanisms for its treatment we pose the inverse problem of shifting the bifurcation points so that they occur at higher values of the bifurcation parameter. In particular, we aim to shift the abscissas of the bifurcation points to $(\gamma_1^*, \gamma_2^*) = 4/3 \times (\gamma_1^0, \gamma_2^0)$. Figure 6 shows the bifurcation diagrams for the system corresponding to the initial kinetic parameters and a perturbation attaining the specified therapeutic goal.

4.2.2 Choice of regularization terms and a numerical evaluation of robustness

As discussed in Sect. 3.2, various choices exist for the regularization term, resulting in different solution properties. Here, we solved 3 instances of the inverse problem taking the following general form:

$$\alpha^* \leftarrow \arg\min_{\alpha \in \mathbb{R}^9} \left\| F(\alpha) - \begin{pmatrix} \gamma_1^* \\ \gamma_2^* \end{pmatrix} \right\|_2^2 + \mu \left\| \frac{\alpha - \alpha^0}{\alpha^0} \right\|_2^2 + \mu_s l_{p,\epsilon} \left(\frac{\alpha - \alpha^0}{\alpha^0} \right).$$

In particular, we consider the following three cases of regularization parameters:

- Case 1: no regularization, $\mu = \mu_s = 0$;
- Case 2: l_2 regularization, $\mu = 0.5$, $\mu_s = 0$;
- Case 3: sparsity regularization, $\mu = 0$, $\mu_s = 0.5$.

Table 3 Identified parameter solutions from the lipoprotein model

Parameter	Nominal	No reg.	l_2 reg.	Sparsity reg.
b	0.1	0.0638	0.0757	0.1000
c	0.05	0.0671	0.0579	0.0873
d	0.0075	0.0539	0.0075	0.0075
d_I	2.0	2.0815	2.0427	2.0002
d_L	0.01	0.1060	0.0100	0.0100
k_I	0.025	0.0925	0.0244	0.0250
k_V	0.3	0.3000	0.3000	0.3000
χ_I	0.1	0.0517	0.0904	0.1000
χ_L	0.6	0.7166	0.5344	0.5999

In particular, the notation $(\alpha - \alpha^0)/\alpha^0$ should be read component-wise, denoting the vector of normalized deviation for the 9 kinetic parameters with respect to the nominal values, α^0. The identified solutions are given in Table 3 and Fig. 7 shows the deviation of identified parameters α^* in comparison to their nominal values. In particular, we note that in the non-regularized case, parameters d_L and d are significantly increased, close to an order of magnitude higher than their nominal values. In comparison, using the l_2 regularization, the identified parameters deviate much less from the nominal values; however the desired shift in the bifurcation diagram is brought about via changes in many parameters. In contrast, using the sparsity approach a single parameter c is identified. Clearly, the identified solutions exhibit different properties with respect to their magnitudes and sparsity; the question naturally arises: how do they differ in robustness?

To numerically estimate robustness in the identified solutions, we examine the resulting perturbations $\{F(\alpha^* + \delta\alpha) - \Gamma^* : \delta\alpha \in \Delta\}$ taking Δ to consist of the set of perturbations in the individual components of the parameter vector. That is, $\Delta = \cup_{i=1}^{m}\{0.5j/N \cdot |\alpha_i^0| \cdot e^i : j \in \mathbb{Z}, -N \leq j \leq N\}$, where we take $N = 20$ number of samples in each direction, e^i denotes the i-th column of the $m \times m$ identity matrix and 0.5 represents the perturbation amplitude. Thus, the same set of parameter variation Δ is introduced in each of the 3 solutions shown in Table 3. For each of the 3 regularization cases considered, we plot the histograms for the variations in the components of the mapped values, $F(\alpha^* + \delta\alpha)$; also shown in the histogram are the corresponding desired values, γ_1^* and γ_2^*. Looking at the results shown in Fig. 8, we first observe that the variability for the unregularized case are higher than that for the regularized cases: for γ_1, the standard deviation for the unregularized case 0.12 versus 0.111 and 0.0916 for the l_2 and sparsity regularization respectively; for the γ_2 results, we have 0.136 versus 0.122 and 0.101 respectively. We remark that the same parameter variation (defined respect to the sizes of the nominal parameters) is used in the variability analysis, hence the differences in the robustness are not due to the shift in the magnitudes of the parameter values. The second observation is that the sparse solution results in less variability than the l_2 case, under the parameter perturbation we considered. While these results were obtained using a particular choice of regularization parameter and carried out on a specific system, it raises the question of

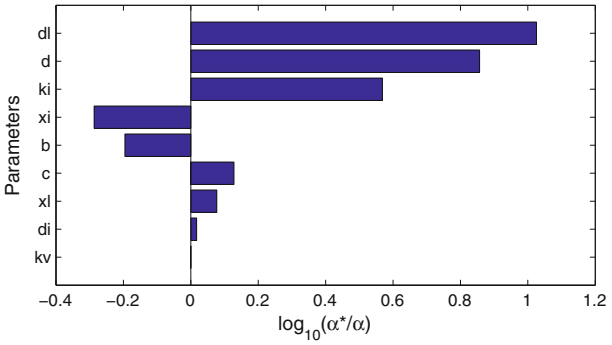

(a) Case 1: no regularization

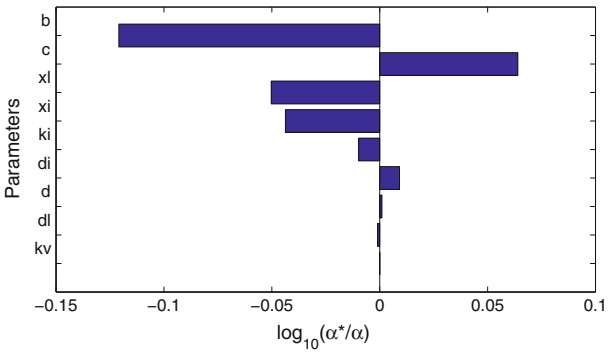

(b) Case 2: l_2 regularization

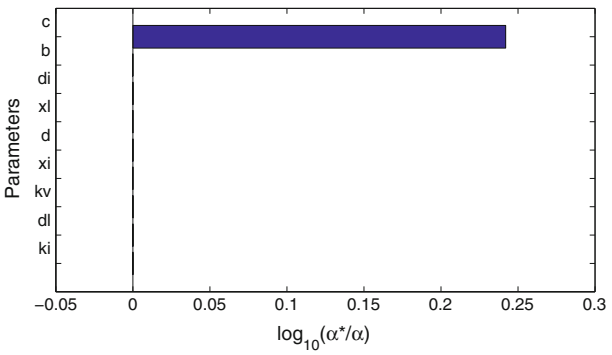

(c) Case 3: sparsity regularization

Fig. 7 Comparison of identified parameters using 3 different strategies. In each of the 3 regularization cases, the logarithmic ratios of identified parameters to their nominal values are plotted

whether regularization by itself could lead to an increase in parametric robustness. If one resorts to solving the robust counterpart of the inverse problem to directly counteract parametric variability, one could further increase the robustness of the identified solution.

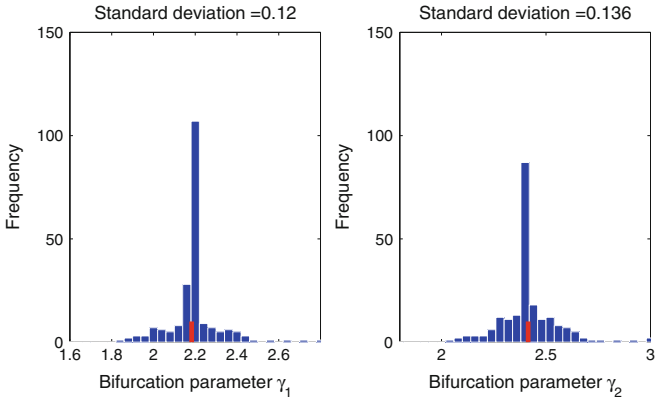

(a) Case 1: no regularization

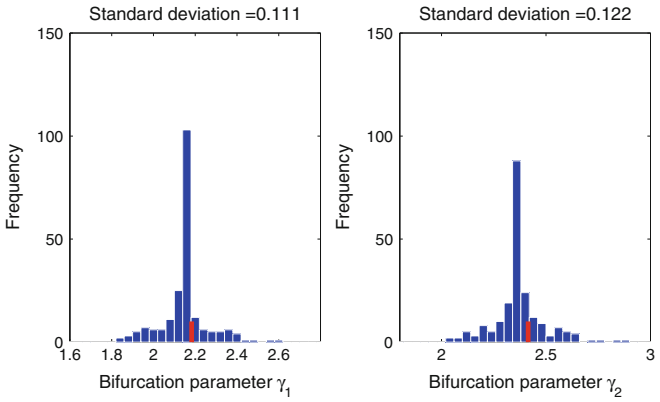

(b) Case 2: l_2 regularization

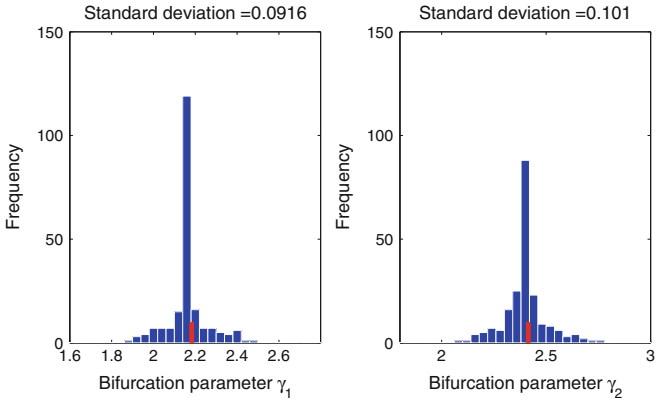

(c) Case 3: sparsity regularization

Fig. 8 Numerical comparison of solution robustness obtained using the 3 different regularization strategies. In each subfigure, the *red bars* indicate the values of γ_1^* and γ_2^* and the computed standard deviations are shown at the *top* of the plots (color figure online)

4.2.3 Certificate for solution robustness

Next, we reformulate the above robustness test as a feasibility problem fulfilling certain positivity conditions. Although testing for positivity of a polynomial function is NP-hard (Murty and Kabadi 1987), recent developments by Parrilo (2003) and Aylward et al. (2008) have explored the use of semidefinite programs (SDPs) to study a relaxation of this problem, namely, to check if a polynomial function can be expressed as a sum of squares (SOS). Clearly, being SOS is only a sufficient (and in some cases quite conservative) condition for positivity but, on the other hand, it is a condition that can be checked with the aid of SDPs (Vandenberghe and Boyd 1996; Parrilo 2005, 2003; Lasserre and Putinar 2010). The key advantage of SDPs is their generality and flexibility together with the fact that they can be solved efficiently using interior-point methods (Vandenberghe and Boyd 1996; Boyd and Vandenberghe 2004; Parrilo 2003). In this paper, we solve SOS programmes using `SOSTOOLS`, (Prajna et al. 2002) a free, third-party `MATLAB` toolbox that relies on the SDP solver `SeDuMi` (Sturm 1999).

Let us suppose the kinetic parameters $b, c, d_I, d_L, k_V, \chi_I, \chi_L$ are fixed at their nominal values as given in Table 3. Let $v^{\mathrm{T}} = [k_I, d]$ be the vector of variable kinetic parameters and v^{sol} correspond to each of the 3 sets of identified values given in Table 3. Consider the parameteric η-box: $\mathcal{V} \equiv \{v \in \mathbb{R}^2 \mid v_i^{sol} \leq v_i \leq v_i^{sol}(1+\eta)\}$. For each of the 3 identified solutions given in Table 3, we would like to construct a certificate ensuring $[LDL] < 3$ for $v \in \mathcal{V}$ and control parameters within the box $0 \leq u_V \leq 1.5$ and $1 \leq d_{IC} \leq 2$. Hence, we formulate the following SOS problem, where state vector $x \in {\mathbb{R}_+}^5$ codes for the five state variables given in (19) and $f(x)$ the corresponding vector field:

$$
\begin{aligned}
&\max_{\substack{\eta \in \mathbb{R}^+ \\ p_1(v), p_2(v) \text{ are SOS} \\ p_3(x,v), p_4(x,v) \text{ are SOS}}} \quad \eta \\
&\text{s. t. } p_1(v)\left(f_1(x)^2 + f_2(x)^2 + f_3(x)^2 + f_4(x)^2 x_5^2 + f_5(x)^2\right) \\
&\quad + (v - v^{sol})^{\mathrm{T}}(v - v^{sol}(1+\eta)) + p_2(v)x_3(x_3 - 3) \\
&\quad + p_3(x,v)u_V(u_V - 1.5) + p_4(x,v)(d_{IC} - 1)(d_{IC} - 2) \text{ is SOS}, \ \forall x, v. \qquad (20)
\end{aligned}
$$

Solving (20) for the 3 cases, we obtain the following values for η : 0.0001514 for the unregularized solution, 0.0066513 for the l_2 regularized solution and 0.008703 for the sparsity regularized case. Hence, we see that for the regularized cases, there is a significantly larger parameter box size for which we can guarantee that $[LDL] < 3$; moreover, the sparse solution results in the largest certified box.

In conclusion, the result of the robustness analysis gives a promising outcome since, as discussed earlier, sparse solutions correspond to the use of only a few drugs in combination for disease treatments. Therefore, sparse solutions are easier to test and possibly minimizing the extent of side effects. Indeed, statins, which belong to a class of drugs used to lower LDL levels, are HMG-CoA reductase inhibitors (Ma et al. 1986), which means that they lower the production rate of VLDL, which is described by the parameter u_V in the model. Additionally, they alter the intracellular cholesterol

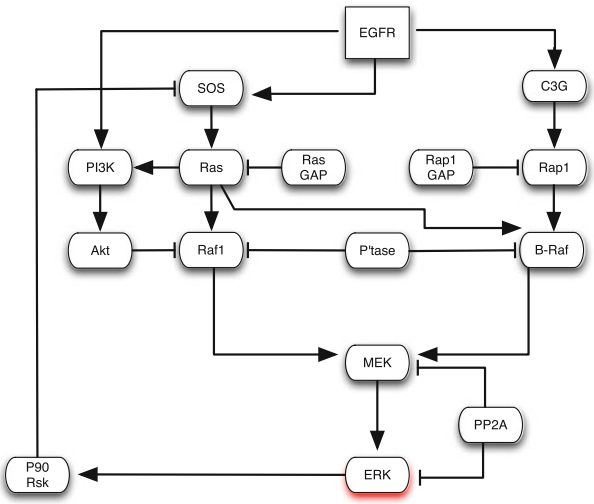

Fig. 9 Schematic diagram of the EGFR signaling network (Orton et al. 2009)

levels in hepatic cells and thus, the value of c in these cells, which is the parameter identified using the sparsity approach.

4.3 EGFR/ERK signaling pathway

The Epidermal Growth Factor Receptor (EGFR) activated Extracellular-signal Regulated Kinase (ERK) pathway plays a critical role in regulating cell proliferation by relaying signal from cell membrane to the nucleus (Orton et al. 2009). In normal cells, Epidermal Growth Factor (EGF) induces a transient activation of ERK; however, upon genetic mutations ERK can become active in a sustained way, leading to cancerous cell proliferation. For a schematic diagram showing how the signal is relayed from EGFR to ERK, refer to Fig. 9. Via computational modeling of the known interactions, it has been shown that mutations in different genes in the pathway lead to distinct perturbations of the signaling pattern.

One particular perturbation known to lead to cancer is a mutation in EGFR so that it is not degraded by the cellular machinery, as would be the case in normal cells. Constitutively active EGFR in turn actives SOS and C3G even in the absence of EGF, which then activate the Ras and Rap1 branches of the pathway. Figure 10 shows the simulation results of the EGFR model as described in Orton et al. (2009), for the normal as well as the cancerous case where the EGFR degradation rate has been set to 0.

Due to the cross-talk between the Ras and Rap1 pathways as well as the negative feedback from ERK to SOS, it is not clear how best to target the network to compensate for the constitutively active EGFR after the mutation. Given our goal of reverting the system back to having a transient activation of ERK, an operator that could differentiate the healthy from the diseased state consist of integrals over

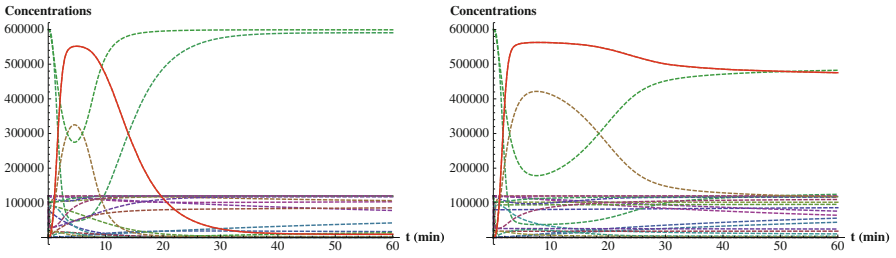

(a) Normal case **(b)** Cancerous case

Fig. 10 Time-course of the EGFR model for normal and cancerous cases, with active ERK shown in *solid red curves* (color figure online)

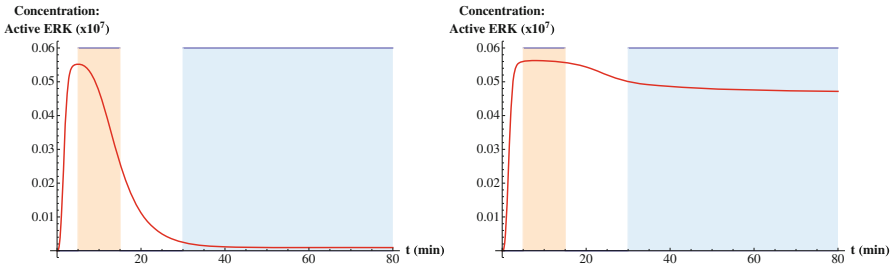

(a) Normal case **(b)** Cancerous case

Fig. 11 Time-course of active ERK and the time window of interest. The area-under-curve (AUC) for the two windows $\mathcal{T}_1$ and $\mathcal{T}_2$ evaluate to 0.46 and 0.05 respectively for normal cells, while they are 0.56 and 2.34 for cancerous cells

the time-windows. Motivated by the solution trajectories shown in Fig. 10, we consider as the forward operator the following normalized time-integrals of the level of active ERK, for the time-intervals from 5 to 15 min and 30 to 80 min respectively:

$$F(\alpha) = \begin{pmatrix} \frac{1}{K}\int_{\mathcal{T}_1} \mathrm{Erk}_{act}(\alpha, t)dt \\ \frac{1}{K}\int_{\mathcal{T}_2} \mathrm{Erk}_{act}(\alpha, t)dt \end{pmatrix}. \tag{21}$$

where $\mathcal{T}_1 = [5, 15]$, $\mathcal{T}_2 = [30, 80]$ and $K = 10^7$ a normalization factor. As illustrated in Fig. 11, we note that while both the normal and cancerous cells have high levels of active ERK in the first window $t \in \mathcal{T}_1$, in the second window $t \in \mathcal{T}_2$ the level is high in cancerous cells but low in the normal cells. In particular, the integrals defined in (21) evaluate to 0.46 and 0.05 in normal cells, while they are 0.56 and 2.34 in cancerous cells. With the set of 54 kinetic parameters in the model as variables, in the cancerous case we wish to identify parameters α^* that would revert system dynamics back to having a transient ERK activation. An examination of the difference between the identified to nominal parameters, $\alpha^* - \alpha^0$, would then suggest the optimal intervention nodes in the signaling network. We solve the following inverse problem, choosing various combinations of values for the regularization parameters μ, μ_s:

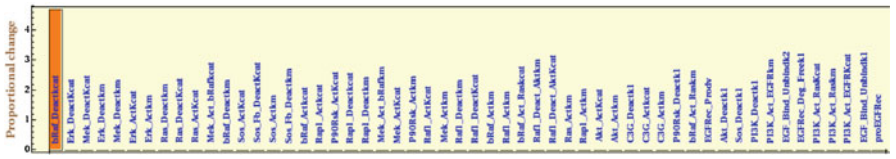

(a) $\mu = 0.04, \mu_s = 0.16$

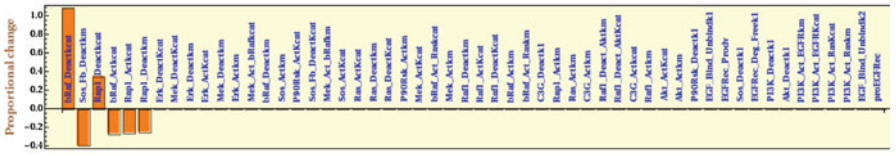

(b) $\mu = 0.08, \mu_s = 0.12$

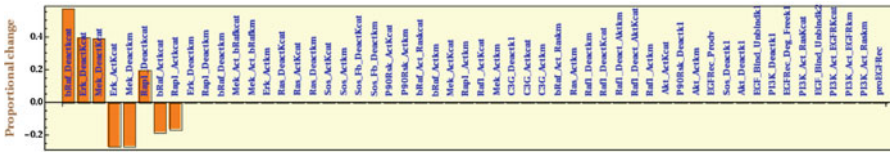

(c) $\mu = 0.12, \mu_s = 0.08$

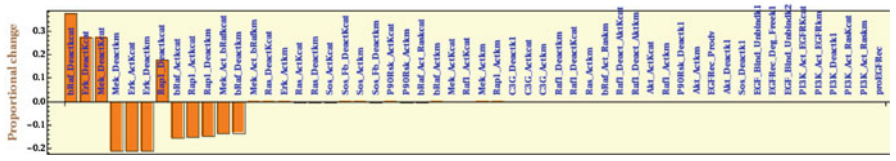

(d) $\mu = 0.16, \mu_s = 0.04$

Fig. 12 Identified parameters reversing the effect of EGFR mutation on ERK activation. A sequence of solutions are obtained using the stated choice of regularization parameters. In each case, the quantity $(\alpha^* - \alpha^0)/\alpha^0$ is plotted

$$\alpha^* \leftarrow \arg\min_{\alpha \in \mathbb{R}^{54}} \left\| F(\alpha) - \begin{pmatrix} 0.5 \\ 0.1 \end{pmatrix} \right\|_2^2 + \mu \left\| \log\left(\frac{\alpha}{\alpha^0}\right) \right\|_2^2 + \mu_s l_{p,\epsilon}\left(\log\left(\frac{\alpha}{\alpha^0}\right)\right). \tag{22}$$

The desired values in the components of the operator $F(\cdot)$ are chosen to be 0.5 and 0.1, as these are the typical values one might observe in normal cells. We use the notational convention that $\log(\cdot)$ is applied component-wise to the vector of parameter ratios. The logarithmic scaling was chosen in order to allow parameters to vary over orders of magnitude if necessary. In terms of implementation, the problem (22) was solved via interior-point optimization method, in which the adjoint-based method (Lu et al. 2008) was used for computing the derivative, $F'(\alpha)$.

The inverse problem (22) was solved using various regularization parameter combinations, ranging from $(\mu, \mu_s) = (0.04, 0.16)$ to $(0.16, 0.04)$. The sequence of identified parameters are shown in Fig. 12. In particular, we see that using $\mu = 0.04$ and $\mu_s = 0.16$, a single parameter is identified: the deactivation rate of B-Raf by

Raf1PPtase. This result indicates that the use of drugs binding to B-Raf and thereby inhibiting it could be a strategy to reverse the effect of EGFR mutation. By increasing the relative weight of l_2 versus sparsity regularization to $\mu = 0.08, \mu_s = 0.12$, we obtained a solution consisting of changing 6 parameters simultaneously: in addition to B-Raf, the solution identifies mechanisms including the deactivation of Rap1 which in turn would also lead to the down-regulation of B-Raf. To summarize, by choosing appropriate weight between the regularization terms, one could attempt to strike the desired balance between sparsity and robustness against resistance mechanisms whereby signals are routed via alternative pathways.

5 Conclusions and outlook

While some of the standard methods and techniques from inverse problems can be directly applied to certain areas of medical diagnosis, new techniques and theories are needed for many of the emerging applications involving mathematical models in systems biomedicine. In particular, the uncertainties that arise at various levels of model description and the lack of available quantitative data pose significantly different challenges than those from other applications of inverse problems in the fields of physical sciences and engineering. Resolving ill-posedness due to the infinite dimensionality of function spaces may not be of as much direct concern in comparison to the need for solving the underlying problems of devising disease treatment strategies in an optimal manner given the constraints on data quantity and quality. Nevertheless, significant mathematical challenges arise in tackling these issues.

While we have proposed some strategies to account for uncertainties and examined some links between regularization strategies and robustness, many important questions remain. One area that we have not touched upon in this paper is uncertainties in kinetic mechanisms and/or network topologies of disease models, due to the incomplete understanding of the underlying biology. For instance, missing out feedbacks and cross-talks in pathways that could occur at significantly different time-scales would likely lead to very contrasting predictions regarding the development of resistance mechanisms in cancer treatments. A consideration of possible missing edges in an existing topology can quickly give rise to combinatorial possibilities regarding network alterations. Quantifying and managing uncertainties in biological models remain important tasks that need to be better addressed for the use of mathematical modeling to increase its utility in understanding diseases and making therapeutic decisions.

References

Acikgoz SU, Diwekar UM (2010) Blood glucose regulation with stochastic optimal control for insulin-dependent diabetic patients. Chem Eng Sci 65(3):1227–1236

Adiels M (2002) A compartmental model for kinetics of apolipoprotein B-100 and triglycerides in $VLDL_1$ and $VLDL_2$ in normolipidemic subjects. Master's thesis, Chalmers University of Technology

August E, Papachristodoulou A (2009) Efficient, sparse biological network determination. BMC Syst Biol 3:25

August E, Parker KH, Barahona M (2007) A dynamical model of lipoprotein metabolism. Bull Math Biol 69:1233–1254

Aylward EM, Parrilo PA, Slotine JJE (2008) Stability and robustness analysis of nonlinear systems via contraction metrics and SOS programming. Automatica 44(8):2163–2170
Ben-Tal A, El Ghaoui L, Nemirovski A (2009) Robust optimization. Princeton Series in applied mathematics. Princeton University Press, Princeton
Ben-Zvi A, Vernon SD, Broderick G (2009) Model-based therapeutic correction of hypothalamic–pituitary–adrenal axis dysfunction. PLoS Comput Biol 5:e1000273
Boyd S, Vandenberghe L (2004) Convex optimization. Cambridge University Press, Cambridge
Cedersund G, Knudsen C (2005) Improved parameter estimation for systems with an experimentally located Hopf bifurcation. Syst Biol (Stevenage) 152:161–168
Converse CA, Skinner ER (1992) Lipoprotein analysis: a practical approach. IRL Press at Oxford University Press, New York
Cooper GM (2000) The cell (a molecular approach), 2nd edn. ASM Press, Boston
d'Aspremont A, El Ghaoui L, Jordan MI, Lanckriet GRG (2007) A direct formulation for sparse PCA using semidefinite programming. SIAM Rev 49(3):434–448
Davidson MH, Jacobson TA (2001) How statins work: the development of cardiovascular disease and its treatment with 3-hydroxy-3-methylglutarylcoenzyme A reductase inhibitor. Cardiol Clin. Medscape, Inc
De Mol C, Mosci S, Traskine M, Verri A (2009) A regularized method for selecting nested groups of relevant genes from microarray data. J Comput Biol 16(5):677–690
Dietschy JM, Gotto AM, Ontko JA (eds) (1978) Disturbances in lipid and lipoprotein metabolism. American Physiological Society, Bethesda
Dietschy JM, Turley SD, Spady DK (1993) Role of liver in the maintenance of cholesterol and low density lipoprotein homeostasis in different animal species, including humans. J Lipid Res 34:1637–1659
Donoho DL (2006) For most large underdetermined systems of equations, the minimal l_1-norm near-solution approximates the sparsest near-solution. Commun Pure Appl Math 59(7):907–934
El Ghaoui L, Lebret H (1997) Robust solutions to least-squares problems with uncertain data. SIAM J Matrix Anal Appl 18(4):1035–1064
Engl HW, Hanke M, Neubauer A (1996) Regularization of inverse problems. Mathematics and its applications, vol 375. Kluwer, Dordrecht
Engl HW, Flamm C, Kügler P, Lu J, Müller S, Schuster P (2009) Inverse problems in systems biology. Inverse Problems 25(12):123014
Faratian D, Goltsov A, Lebedeva G, Sorokin A, Moodie S, Mullen P, Kay C, Um IH, Langdon S, Goryanin I, Harrison DJ (2009) Systems biology reveals new strategies for personalizing cancer medicine and confirms the role of PTEN in resistance to trastuzumab. Cancer Res 69:6713–6720
Glass L, Mackey MC (1979) Pathological conditions resulting from instabilities in physiological control systems. Ann NY Acad Sci 316:214–235
Glass CK, Witztum JL (2001) Atherosclerosis: the road ahead. Cell 104:503–516
Goldstein JL, Brown MS (1977) The low-density lipoprotein pathway and its relation to atherosclerosis. Ann Rev Biochem 46:897–930
Gupta S, Aslakson E, Gurbaxani BM, Vernon SD (2007) Inclusion of the glucocorticoid receptor in a hypothalamic pituitary adrenal axis model reveals bistability. Theor Biol Med Model 4:8
Hafner M, Koeppl H, Hasler M, Wagner A (2009) 'Glocal' robustness analysis and model discrimination for circadian oscillators. PLoS Comput Biol 5:e1000534
Hafner M, Petrov T, Lu J, Koeppl H (2011) Rational design of robust biomolecular circuits: from specification to parameters. In: Koeppl H, Densmore D, Setti G, di Bernardo M (eds) Design and analysis of biomolecular circuits. Springer, Berlin pp 253–279
Iadevaia S, Lu Y, Morales FC, Mills GB, Ram PT (2010) Identification of optimal drug combinations targeting cellular networks: integrating phospho-proteomics and computational network analysis. Cancer Res 70:6704–6714
Kuznetsov YA (2004) Elements of applied bifurcation theory. Applied mathematical sciences, vol 112, 3rd edn. Springer, New York
Lasserre JB, Putinar M (2010) Positivity and optimization for semi-algebraic functions. SIAM J Optim 20(6):3364–3383
Libby P (2002) Atherosclerosis: the new view. Scientific American pp 46–55
Lim CC, Teo KL (1989) A stochastic optimal control approach to a mathematical drug administration model. Math Comput Model 12(8):1009–1015
Liu ET, Lauffenburger DA (2009) Systems biomedicine: concepts and perspectives. Elsevier, Burlington

Lu J (2009) Inverse eigenvalue problems for exploring the dynamics of systems biology models. Adv Appl Math Mech 1(6):711–728
Lu J, Engl HW, Schuster P (2006) Inverse bifurcation analysis: application to simple gene systems. Algorithms Mol Biol 1:11
Lu J, Müller S, Machné R, Flamm C (2008) SBML ODE solver library: extensions for inverse analysis. In: Proceedings of WCSB 2008, Leipzig, Germany
Ma PTS, Gil G, Südhof TC, Bilheimer DW, Goldstein JL, Brown MS (1986) Mevinolin, an inhibitor of cholesterol synthesis, induces mRNA for low density lipoprotein receptor in livers of hamsters and rabbits. PNAS 83:8370–8374
Magombedze G, Garira W, Mwenje E, Bhunu CP (2011) Optimal control for HIV-1 multi-drug therapy. Int J Comput Math 88(2):314–340
Mathews CK, van Holde KE, Ahern KG (2000) Biochemistry. Addison Wesley Longman, San Francisco
Miao H, Xia X, Perelson AS, Wu H (2011) On identifiability of nonlinear ODE models and applications in viral dynamics. SIAM Rev: Soc Ind Appl Math 53(1):3–39. doi:10.1137/090757009
Murty KG, Kabadi SN (1987) Some NP-complete problems in quadratic and nonlinear programming. Math Program 39:117–129
Orton RJ, Adriaens ME, Gormand A, Sturm OE, Kolch W, Gilbert DR (2009) Computational modelling of cancerous mutations in the EGFR/ERK signalling pathway. BMC Syst Biol 3:100
Packard CJ, Demant T, Stewart JP, Bedford D, Caslake MJ, Schwertfeger G, Bedynek A, Shepherd J, Seidel D (2000) Apolipoprotein B metabolism and the distribution of VLDL and LDL subfractions. J Lipid Res 41:305–317
Parrilo PA (2003) Semidefinite programming relaxations for semialgebraic problems. Math Program Ser B 96:293–320
Parrilo PA (2005) Structured semidefinite programs and semialgebraic geometry methods in robustness and optimization. PhD thesis, California Institute of Technology, Pasadena, California
Prajna S, Papachristodoulou A, Parrilo PA (2002) SOSTOOLS—sum of squares optimization toolbox, user's guide. http://www.cds.caltech.edu/sostools
Rodríguez JEFB, Herrera JAC, Tusiente NT, Andino AB, Vilaú F (1999) Aterosclerosis, colesterol y pared arterial: Algunas reflexiones. Rev Cubana Invest Biomed 18(3):169–175
Shimamura T, Imoto S, Yamaguchi R, Fujita A, Nagasaki M, Miyano S (2009) Recursive regularization for inferring gene networks from time-course gene expression profiles. BMC Syst Biol 3:41
Stengel RF (1986) Stochastic optimal control. A Wiley-Interscience Publication. John Wiley and Sons Inc., Wiley, New York
Sturm JF (1999) Using SeDuMi 1.02, a MATLAB toolbox for optimization over symmetric cones. Optim Methods Softw 11–12:625–653. http://sedumi.ie.lehigh.edu
Swan GW (1984) Applications of optimal control theory in biomedicine. Monographs and textbooks in pure and applied mathematics, vol 81. Marcel Dekker Inc, New York
Vandenberghe L, Boyd S (1996) Semidefinite programming. SIAM Rev 38(1):49–95
Velez DA, Mayberg MR, Ludlam WH (2007) Cyclic Cushing syndrome: definitions and treatment implications. Neurosurg Focus 23:E4; (discussion E4a)
White DA, Baxter M (1984) Hormones and metabolic control. Edward Arnold Ltd, London
Yang K, Bai H, Ouyang Q, Lai L, Tang C (2008) Finding multiple target optimal intervention in disease-related molecular network. Mol Syst Biol 4:228
Zarzer CA (2009) On Tikhonov regularization with non-convex sparsity constraints. Inverse Problems 25(2):1–13
Zenker S, Rubin J, Clermont G (2007) From inverse problems in mathematical physiology to quantitative differential diagnoses. PLoS Comput Biol 3(11):2072–2086
Zou H, Hastie T (2005) Regularization and variable selection via the elastic net. J R Stat Soc Ser B Stat Methodol 67(2):301–320